Molecular Devices

DOI: 10.1002/ange.200604397

# Single-Crystal Organic Nanowires of Copper–Tetracyanoquinodimethane: Synthesis, Patterning, Characterization, and Device Applications**

*Kai Xiao,* Jing Tao, Zhengwei Pan, Alex A. Puretzky, Ilia N. Ivanov, Stephen J. Pennycook, and David B. Geohegan**

Single-crystal, one-dimensional semiconductor nanostructures are very important building blocks for nanoscale optical and electronic devices.[1] Currently, much attention is focused on inorganic materials, such as carbon nanotubes[2] and inorganic oxide nanowires,[3] whose properties endow them with considerable potential. Fewer studies have been performed on organic semiconductor nanowires, despite their widespread development for inexpensive organic thin-film optoelectronic devices.[4] Organic semiconducting materials comprised of smaller molecules normally have conjugated structures. As a consequence of their diversity, tailorability, multifunctionality, and ease in forming very highly ordered crystals, it is highly desirable to synthesize single-crystal organic semiconducting nanowires from small molecular compounds,[5] which could serve as low-cost, high-performance building blocks for the next-generation lightweight displays and for applications in information storage.

Copper–tetracyanoquinodimethane (Cu–TCNQ) is a widely studied organic semiconductor because of its capability for reversible, bistable switching of conductivity from a high to a low state through induction by an electric field or optical excitation.[6] Bulk and thin-film forms of Cu–TCNQ have been widely studied,[7] and thus far various methods for the fabrication of Cu–TCNQ nanostructures have been reported, such as vacuum vapor deposition,[8] solution processes in organic solvents,[9] as well as chemical and electrochemical reduction of TCNQ in the presence of metallic Cu or Cu$^+$ ions.[10] However, the use of these techniques to fabricate micro- and nanoscale Cu–TCNQ structures have resulted in significant drawbacks with respect to the yield, size, phase, material multiplicity, production of high-density arrays, and ability to achieve patterned structures. Herein we report the synthesis and patterning of single-crystal semiconductor Cu–TCNQ nanowires by a low-temperature vapor–solid route. The advantage of this synthetic route lies in its simplicity and mild reaction conditions, as well as the high crystallinity of the nanowires grown in the arrays. To demonstrate the potential of the technique we report the design, fabrication, and characteristics of cross-point nonvolatile memory devices based on a network of organic single-crystal nanowires on a flexible poly(ethylene terephthalate) (PET) flexible substrate.

Cu–TCNQ organic nanowires were grown in a controllable manner from reactions of a Cu thin film and TCNQ vapor at low temperatures (Figure 1). The diameters of the nanowires range from 20 to 100 nm, while the lengths could be varied between 1 μm and 20 μm by adjusting the growth time and thickness of the Cu film. There are several important features of these Cu–TCNQ nanowires. First, the nanowires initially grow directly from the patterned Cu film on the substrate surface and make good mechanical connections to the untreated Cu layer, an essential starting point for good electrical connections to device electrodes (Figure 1 a). As the nanowires grow longer, they curve to form a network of nanowires (Figure 1 b). Second, Cu–TCNQ nanowires can be synthesized at temperatures as low as 120 °C by using a simple chemical vapor deposition (CVD) method. Therefore, Cu–TCNQ nanowires can be grown on some temperature-sensitive substrates, such as glass and flexible plastics, which is promising for large-area, low-cost flexible electronic applications. Third, as a result of the vapor–solid reaction growth, the nanowires grow only in areas patterned with Cu thin films and readily yield patterned nanowires. The direction of the nanowires can be influenced by carefully exposing regions of the Cu thin film. Various techniques, such as electron-beam lithography and photolithography, can be used to create patterned Cu films for subsequent growth of Cu–TCNQ nanowires. SEM studies reveal massive growth of fine, long,

---

[*] Dr. K. Xiao, Dr. Z. Pan, Dr. A. A. Puretzky, Dr. I. N. Ivanov,
Dr. D. B. Geohegan
Center for Nanophase Materials Sciences
Oak Ridge National Laboratory
1 Bethel Valley Road, Oak Ridge, TN 37831-6030 (USA)
Fax: (+1) 865-574-4143
E-mail: xiaok@ornl.gov
geohegandb@ornl.gov

Dr. J. Tao, Dr. A. A. Puretzky, Dr. I. N. Ivanov, Dr. S. J. Pennycook,
Dr. D. B. Geohegan
Materials Science and Technology Division
Oak Ridge National Laboratory
1 Bethel Valley Road, Oak Ridge, TN 37831-6030 (USA)

[**] The authors gratefully acknowledge P. Fleming for technical assistance, and H. N. Lee for helpful discussions. We also thank Dr. Z. Zhou for writing the program for the write-read-erase cycle measurements. This research was conducted at the Center for Nanophase Materials Sciences, which is sponsored at the Oak Ridge National Laboratory by the Division of Scientific User Facilities, US Department of Energy. HRTEM and SEAD analyses (J.T. and S.J.P., respectively) were funded by the Division of Materials Sciences and Engineering, Office of Basic Energy Sciences, US Department of Energy under contract DE-AC05-00OR22725 with the Oak Ridge National Laboratory, managed and operated by UT-Battelle, LLC.

Supporting information for this article is available on the WWW under http://www.angewandte.org or from the author.

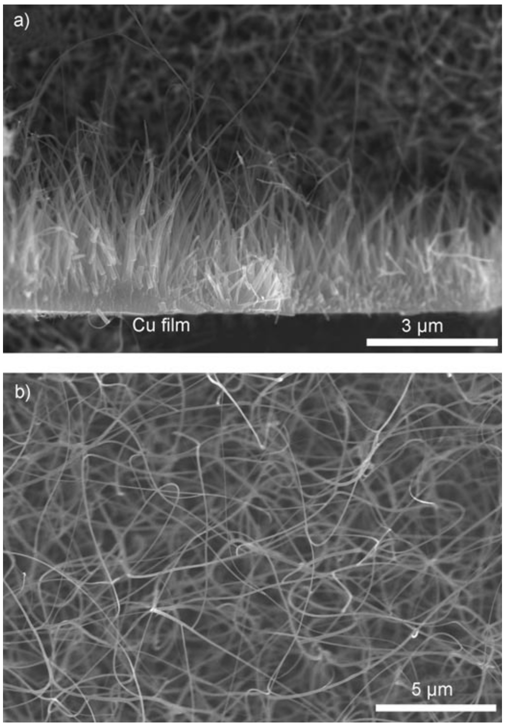

***Figure 1.*** SEM images of Cu–TCNQ nanowires prepared on the Si substrate coated with an approximately 50-nm thick Cu film at 120 °C in an argon flow for: a) 1 h (side view) and b) 2 h (top view).

and flexible Cu–TCNQ nanowires from the Cu thin film patterned with quadrangles (Figure 2 a). The wire growth conforms with high fidelity to the quadrangle shape of the Cu film. Figure 2 b, c, and d show SEM images of Cu–TCNQ nanowires grown from patterned Cu lines and nanodots on a Si substrate. Selective growth of the nanowires can be readily seen. It is clear that nanowires grow only from regions that are coated with Cu, thus making it possible to pattern arrays of Cu–TCNQ nanowires into designs for their integration into devices with large numbers of parallel nanowires.[11]

Raman spectroscopy has often been used to identify the vibrational modes resulting from different chemical bonds between metal atoms and TCNQ molecules in metal–TCNQ complexes.[12] Figure 3 shows the Raman spectrum of as-grown Cu–TCNQ nanowires and TCNQ thin films. The characteristic principal vibration modes at 1202 $\text{cm}^{-1}$ (C=CH bending), 1380 $\text{cm}^{-1}$ (C−CN wing stretching), 1603 $\text{cm}^{-1}$ (C=C ring stretching), and 2208 $\text{cm}^{-1}$ (C−N stretching) confirm that the nanowires are Cu–TCNQ. However, some of the principal vibration modes of Cu–TCNQ nanowires—at 1450 $\text{cm}^{-1}$ (C−CN wing stretch) and 2225 $\text{cm}^{-1}$ (C−N stretch)—expected on the basis of data reported for TCNQ films,[12] are, in fact, red-shifted by 70 $\text{cm}^{-1}$ and 17 $\text{cm}^{-1}$, respectively. According to the previous studies, this decrease in the vibrational energy can be attributed to charge transfer between atomic Cu and free TCNQ.[12]

Detailed structural characterization of the Cu–TCNQ nanowires was achieved by transmission electron microscopy (TEM, Figure 4). Cu–TCNQ nanowires were grown directly on a copper grid by the same growth procedure as described

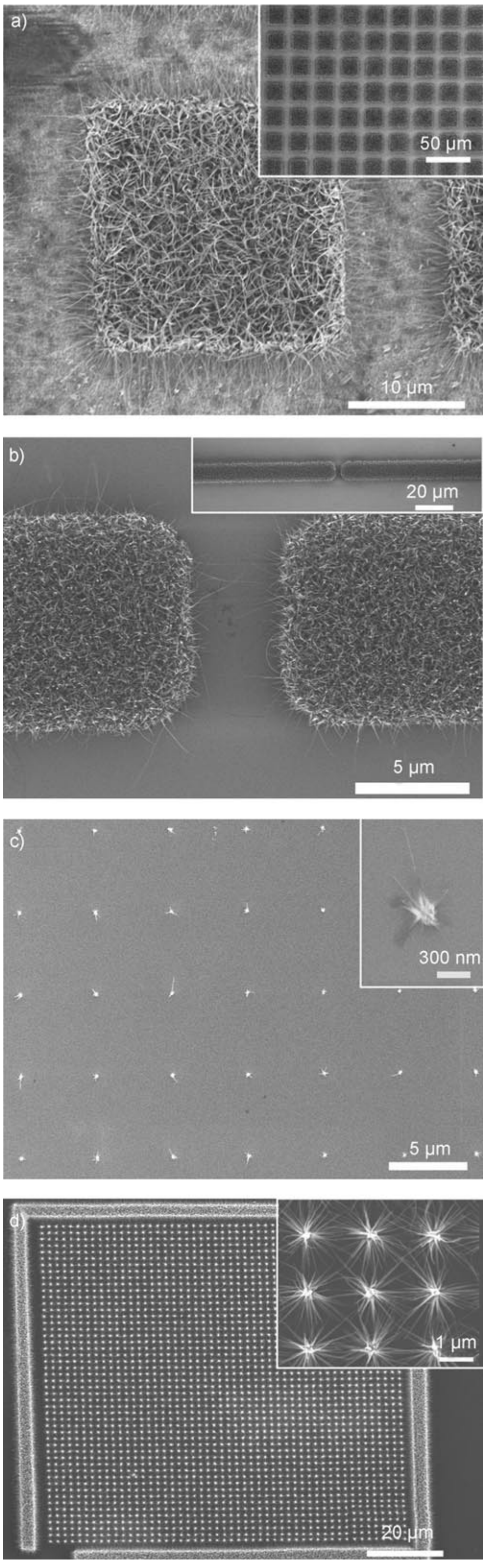

***Figure 2.*** SEM images of patterned Cu–TCNQ nanowires on a Si substrate. a) Nanowires patterned in quadrangles. b) Nanowires patterned in lines. c) Nanowires grown from patterned 100 nm dots of Cu. d) Nanowires grown from patterned 300 nm dots of Cu. The inset of (a) and (b) show low magnification SEM images. The inset of (c) and (d) show magnified SEM images, which reveals the nanowires within each patterned Cu pad.

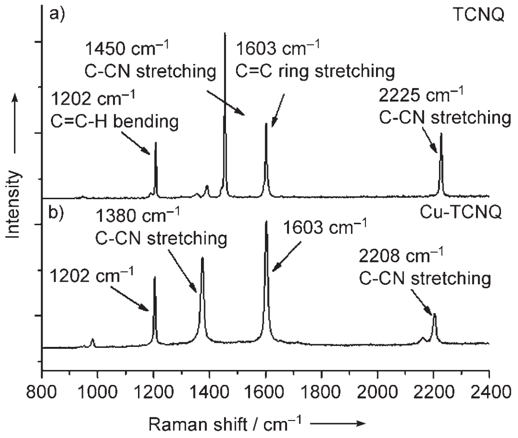

***Figure 3.*** Micro-Raman spectra of the TCNQ film (a) and the Cu–TCNQ nanowires (b). Charge transfer causes a shift of the vibrational modes at 1450 and 2225 $\text{cm}^{-1}$.

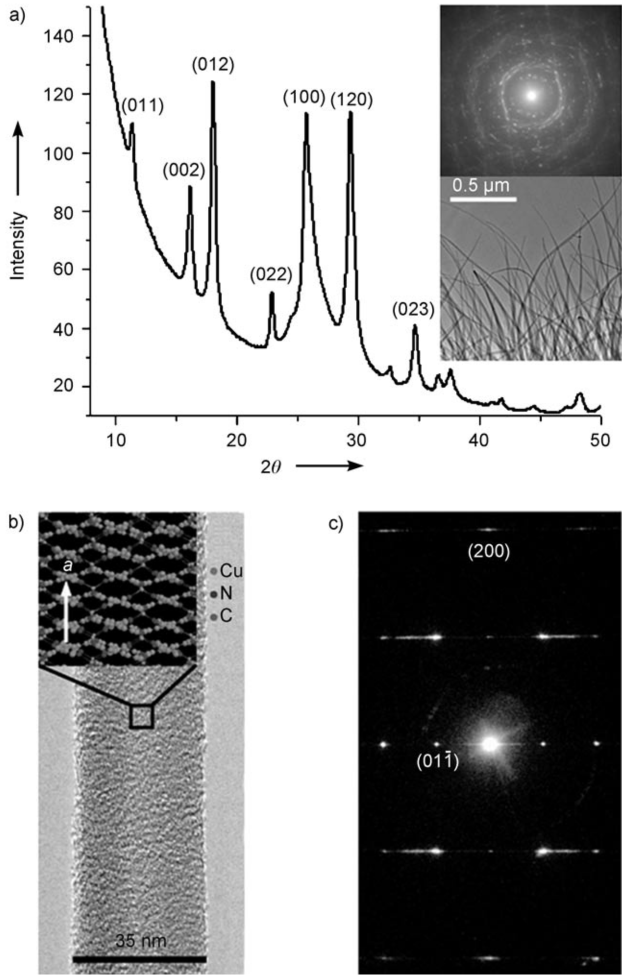

***Figure 4.*** Structural characterization of the Cu–TCNQ nanowires by TEM. a) The integrated intensity of the SAED is shown as a function of the reflection angle, with the major reflections indexed. The two insets show the SAED pattern obtained from a collection of the nanowires (top) and the TEM image of the nanowires from the copper edge to vacuum (bottom). b) An example of a TEM image of an individual Cu–TCNQ nanowire. The inset above the nanowire demonstrates the stacking of the *bc* planes along the *a*-axis direction. c) The SAED pattern along [011] zone axes taken from the individual nanowire shown in (b).

above. The two insets in Figure 4a show the TEM image of the nanowires protruding from the copper edge of the grid (the lower inset) and the selected-area electron diffraction (SAED) pattern obtained from a collection of the nanowires (the upper inset). The diameters of the nanowires are not constant: they taper from a basal dimension of 150 nm to 30 nm at their tips. The diffraction intensity is, however, not uniform over certain azimuthal angles in the SAED pattern, thus indicating the existence of a preferential orientation or textural structure in the Cu–TCNQ nanowires. The integrated intensity of the SAED pattern as a function of the reflection angle is shown in Figure 4a, with the major reflections indexed. The presence of just one set of sharp peaks in the plot indicates a single Cu–TCNQ phase in the nanowires. The unit-cell parameters of $a = 3.89$, $b = 11.27$, and $c = 11.27$ Å measured from the SAED patterns of the Cu–TCNQ nanowires are in good agreement with the literature values of bulk Cu–TCNQ phase I with a monoclinic unit cell.[7]

Figure 4b shows a TEM image of an individual Cu–TCNQ nanowire with a diameter of 35 nm. The SAED pattern taken from this nanowire is shown in Figure 4c and shows a single-crystalline pattern that can be indexed as the [011] zone of the crystal structure of Cu–TCNQ phase I.[7] The SAED patterns from individual Cu–TCNQ nanowires were indexed and most were single crystals along the [011] or [010] zone axis. This finding strongly suggests that the growth direction is along the *a*-axis of the monoclinic Cu–TCNQ phase I structure, which corresponds to stacked Cu–TCNQ molecules with a large $\pi$–$\pi$ overlap. The top inset in Figure 4b shows the derived structural model of the stacking of the *bc* planes along the *a*-axis direction of the Cu–TCNQ organic nanowires based upon the SAED data. The strong $\pi$–$\pi$ stacking of the Cu–TCNQ molecules along the *a*-axis direction favors the one-dimensional growth of the crystalline nanowire. This $\pi$–$\pi$ stacking may enhance the charge-carrier mobility, which is believed to be favored along this direction.[13]

The growth of the Cu–TCNQ nanowires was investigated by SEM, Raman microscopy, and TEM. SEM images of Cu–TCNQ nanowires grown for different times (see the Supporting Information) show that the nanowires do not nucleate immediately, but begin to form up to 30 minutes after the introduction of TCNQ vapor to the Cu surface. During this time, layers of Cu–TCNQ film form on the Cu surface by chemical reaction[14] (confirmed by Raman analysis, see the Supporting Information). Subsequently, islands of Cu–TCNQ appear and form the nuclei for subsequent, rapid growth of the nanowires. The presence of Cu throughout the nanowire and the absence of particles at the tips of the nanowires imply a base-growth mechanism through a vapor–solid reaction. In this model, Cu from the predeposited film or TCNQ vapor arriving on the substrate diffuse through the base of the growing Cu–TCNQ nanowire. The diffusion of Cu through growing 200-nm-thick Cu–TCNQ films has been previously observed[14] (and also observed here, see the

Supporting Information). These experiments lend support to diffusion driven by chemical potentials in the base-growth of Cu–TCNQ nanowires; however, further work is necessary to clarify the growth mechanism and the evolution of the nanostructure morphology observed in these experiments.

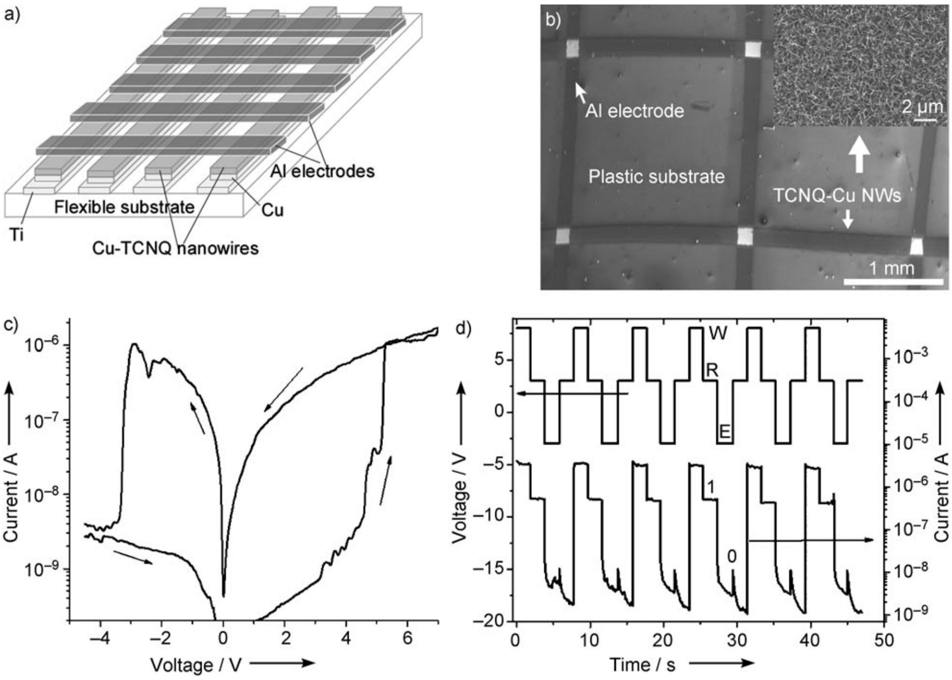

***Figure 5.*** Nanowire network cross-point memory device on plastic substrate. a) Schematic representation of a cross-point memory device. b) SEM image of the cross-point memory device. The inset shows the SEM image of the network of Cu–TCNQ nanowires grown on the plastic substrate. c) The typical *I*/*V* curves of the cross-point memory device with the network of Cu–TCNQ nanowires. d) Write-read-erase cycles of the device. The top and bottom traces are the applied voltage and the corresponding current response, respectively. W, R, and E in the top trace correspond to write, read, and erase, respectively. “1” and “0” in the bottom trace indicate the device is in the high and low conductivity state, respectively.

The low-temperature vapor-phase process to generate Cu–TCNQ organic nanowires makes it possible to fabricate them selectively on temperature-sensitive plastic substrates. We have used this approach to fabricate a cross-point organic memory device on a plastic substrate by using an organic nanowire network. The device has a simple structure, with a network of Cu–TCNQ nanowires sandwiched between the bottom Cu/Ti electrode and a top Al electrode (Figure 5 a,b). The *I*/*V* curve of the best device is shown in Figure 5 c. Starting with a negative voltage, the devices were first in the OFF state. After reaching a sufficient positive voltage, the memories switched to a high conductive ON state. The conductivity of the device in the ON state was more than two orders of magnitude larger than that in the OFF state (it is worth noting that this ON/OFF ratio is the highest measured in our study, but that ON/OFF ratios between 10:1 and 100:1 are routinely achieved on our devices). The high-conductivity state returns to the low-conductivity state through the application of a sufficient negative bias. Consequently, the switching behavior leads to a pronounced hysteretic *I*/*V* feature with two different states. Electrical switching of the device was performed numerous times (Figure 5 d). These results demonstrate the nonvolatile nature of the memory effect in the network of Cu–TCNQ nanowires. The device was sequentially written, read, and erased more than ten times before several memory elements of this prototype failed. The most often observed failure mode is that a memory can no longer be turned OFF after cycling. Further work is underway to optimize the growth of the Cu–TCNQ nanowires to improve the cycling to the OFF state and fully elucidate the switching mechanisms, which may be a field-induced electrochemical reaction[15] or a structural phase change.[7]

In summary, we have shown that high-quality, single-crystal organic semiconductor Cu–TCNQ nanowires can be synthesized and patterned on various substrates (such as, silicon, glass, and flexible plastic) at low temperatures (<120 °C). The Cu–TCNQ nanowires grow preferentially along the [100] direction of the monoclinic Cu–TCNQ phase I structure, which coincides with the direction of strong π–π stacking of Cu–TCNQ molecules. A cross-point memory device based on a network of Cu–TCNQ nanowires has been demonstrated and switched electrically between two states with a conductivity difference of more than two orders of magnitude. The device exhibited nonvolatile electrical properties. Thus, the low-temperature synthesis and patterning of single-crystal Cu–TCNQ nanowires directly on flexible substrates may enable the fabrication of cross-point memory devices which could have an important impact on low-cost, flexible electronics and high-density information storage applications.

Received: October 26, 2006

**Keywords:** chemical vapor deposition · electron microscopy · molecular devices · nanostructures · organic semiconductors

[1] H. Dai, E. W. Wong, C. M. Lieber, *Science* **1996**, *272*, 523; D. Wang, H. Dai, *Angew. Chem.* **2002**, *114*, 4977; *Angew. Chem. Int. Ed.* **2002**, *41*, 4783.
[2] P. Avouris, *MRS Bull.* **2004**, *29*, 403.
[3] P. Yang, H. Yan, S. Mao, R. Russo, J. Johnson, R. Saykally, N. Morris, J. Pham, R. He, H. Choi, *Adv. Funct. Mater.* **2002**, *12*, 323.
[4] C. D. Dimitrakopoulos, D. J. Mascaro, *IBM J. Res. Dev.* **2001**, *45*, 11; J. Ouyang, C. W. Chu, C. R. Szmanda, L. Ma, Y. Yang, *Nat.*

*Mater.* **2004**, *3*, 918; N. S. Sariciftci, L. Smilowitz, A. J. Heeger, F. Wudl, *Science* **1992**, *258*, 1474.

[5] A. C. Grimsdale, K. Müllen, *Angew. Chem.* **2005**, *117*, 5732; *Angew. Chem. Int. Ed.* **2005**, *44*, 5592; S. Xiao, J. Tang, T. Beetz, X. Guo, N. Tremblay, T. Siegrist, Y. Zhu, M. Steigerwald, C. Nuckolls, *J. Am. Chem. Soc.* **2006**, *128*, 10700.

[6] M. R. Bryce, L. C. Murphy, *Nature* **1984**, *309*, 119; R. S. Potember, T. O. Poehler, R. C. Benson, *Appl. Phys. Lett.* **1982**, *41*, 548.

[7] R. A. Heintz, H. Zhao, X. Ouyang, G. Grandinetti, J. Cowen, K. R. Dunbar, *Inorg. Chem.* **1999**, *38*, 144; S. Sun, P. Wu, D. Zhu, *Thin Solid Films* **1997**, *301*, 192.

[8] G. Cao, C. Ye, F. Fang, X. Xing, H. Xu, D. Sun, G. Chen, *Micro* **2005**, *36*, 267.

[9] Y. Liu, Z. Ji, Q. Tang, L. Jiang, H. Li, M. He, W. Hu, D. Zhang, L. Jiang, X. Wang, C. Wang, Y. Liu, D. Zhu, *Adv. Mater.* **2005**, *17*, 2953.

[10] K. Neufeld, A. P. O'Mullane, A. M. Bond, *J. Am. Chem. Soc.* **2005**, *127*, 13846.

[11] K. Xiao, I. N. Ivanov, A. A. Puretzky, Z. Liu, D. B. Geohegan, *Adv. Mater.* **2006**, *18*, 2184.

[12] E. I. Kamitsos, C. H. Tzinis, W. M. Risen, *Solid State Commun.* **1982**, *42*, 561.

[13] K. Balakrishnan, A. Datar, R. Oitker, H. Chen, J. Zuo, L. Zang, *J. Am. Chem. Soc.* **2005**, *127*, 10496.

[14] P. Liu, Y. Jiang, H. Xie, F. Guo, J. Li, *Jpn. J. Appl. Phys.* **2005**, *16*, L494; D. Wöhrle, R. Benters, O. Suvorova, G. Schnurpfeil, N. Trombach, T. Bogdahn-rai, *J. Porphyrins Phthalocyanines* **2000**, *4*, 491.

[15] R. S. Potember, T. O. Poehler, D. O. Cowan, *Appl. Phys. Lett.* **1979**, *34*, 405.